Can Immunoglobulin C_H1 Constant Region Domain Modulate Antigen Binding Affinity of Antibodies?

Otto Pritsch,* Gilbert Hudry-Clergeon,‡ Malcolm Buckle,§ Yves Pétillot,‡ Jean P. Bouvet,‖ Jean Gagnon,‡ and Guillaume Dighiero*

**Unité d'Immunohématologie et d'Immunopathologie, Institut Pasteur, 75724 Paris cedex 15, France; ‡Institut de Biologie Structurale Jean-Pierre Ebel, CEA-CNRS, 38027 Grenoble cedex 1, France; §Unité de Physicochimie des Macromolécules Biologiques, Institut Pasteur, 75724 Paris cedex 15, France; and ‖Unité d'Immunocytochimie, Institut Pasteur, 75724 Paris cedex 15, France*

Abstract

Although the switch process is frequently associated with affinity maturation, the constant region is not assumed to play a role in Ag–Ab binding. In the present work, we demonstrate that two clonally related human monoclonal Igs sharing identical V_H and V_L sequences, but expressing different isotypes ($IgA1\kappa^{PER}$ and $IgG1\kappa^{PER}$), bind tubulin with significantly different affinities. This difference was mainly accounted for by a disparity in the association rate constants. These results suggest that affinity maturation of this clone could be achieved through class switching in the absence of further somatic mutations. Since the differences observed were found at the Fab level, they also suggest a role for the C_H1 domain in structuring the Ag-binding site into a more kinetically competent form. (*J. Clin. Invest.* 1996. 98:2235–2243.) Key words: immunoglobulins • isotype • switching • C_H1 • affinity

Introduction

Ig are heterodimeric proteins composed of two H and two L chains. Each L chain contains either a C_κ or a C_λ and a V_L domain that helps define the Ag-binding site of the Ab. In addition to a variable domain, each H chain contains between three and four constant domains that specify the effector function of the Ab. Multisequence comparisons of variable domains have shown that each variable domain contains three regions of extensive sequence variability, termed the complementary determining regions (CDRs),[1] and four regions of relative sequence stability, termed framework regions (FRs). The three L chain CDRs and the three H chain CDRs are juxtaposed to form the Ag-binding site of the Ab, as classically defined. In turn, the FRs create a scaffold that surrounds, supports, and influences the conformation and structure of the CDRs (1–4).

There are five major classes of C_H domains in a mammalian genome (μ, δ, γ, ϵ, and α). B cells are endowed with the ability to switch from one set of constant domains to another (1). This class switch allows the B cell to change the effector function of the Ab that it produces while maintaining the Ag specificity of the original Ab (5). The sequence and structure of the Ag binding site can be altered through a process of somatic hypermutation that is targeted at the V domain, leading to a change in the binding affinity and specificity of the Ab (2, 3, 6, 7). Both class switching and somatic hypermutation of the variable domains are processes that occur in the germinal center B cells that are undergoing Ag selection and affinity maturation of their Ab. It has long been assumed that the constant domains do not play a role in the maturation of Ag–Ab interactions. However, recent studies have reported the influence of Fc on apparent binding strength, particularly among IgG subclasses, which do not depend on multimerization, but on subtle Fc–Fc cooperative interactions (8, 9).

We have previously described in a single individual, the presence of four different clonally related MIg in the serum of a patient suffering from an immunocytic sarcom (10). Three of these MIg were found to bind tubulin. Among these, $IgG1\kappa^{PER}$ was found to bind tubulin and to display binding with actin, myosin, and ssDNA, whereas $IgA1\kappa^{PER}$ and $IgG4\kappa^{PER}$ were found to exclusively bind tubulin. In the present work, we have further studied two of these ($IgG1\kappa^{PER}$ and $IgA1\kappa^{PER}$) and demonstrated that, despite sharing identical variable H and L sequences, these Ab and their Fab fragments bind tubulin with significantly different affinities, suggesting that the C_H1 constant domain may play a role in defining the Ag–Ab affinity.

Methods

Purification of MIg

MIg^{PER} were purified from patient's serum by ammonium sulfate precipitation, followed by ion-exchange chromatography on a DE-52 column (Whatman, Maidstone, UK). Two different IgG of the γ_1 and γ_2 subclasses were eluted from the DE-52 column at the same molarity (0.005 M), and were further isolated by preparative isoelectrofocusing with a Rotafor apparatus (Bio-Rad Laboratories, Richmond, CA). Monomeric and dimeric $IgA1\kappa^{PER}$ were eluted in 0.03 and 0.05 M fractions, respectively. Purity, homogeneity, and M_r of the $IgG1\kappa^{PER}$ and $IgA1\kappa^{PER}$ fractions were then assessed by ELISA and by HPLC, as described (10). The pI of the different MIg was measured by isoelectrofocusing.

Preparation of Fab and F(ab')2 fragments from $IgG1\kappa^{PER}$ and $IgA1\kappa^{PER}$

To obtain purified Fabγ fragments, 3 mg of monoclonal $IgG1\kappa^{PER}$ were digested for 24 h at 37°C with 50 μg of papain in the presence of the reducing agent cystein. The reaction was terminated by adding crystalline iodoacetamide to a 0.03 M final concentration. Separation of Fab from Fc fragments was assessed by ion-exchange chromatography in a Trisacryl-DEAE column equilibrated with 0.01 M Tris-HCl, pH 8.6, and eluted with a linear gradient from 0 to 0.5 M NaCl in the

Address correspondence to Guillaume Dighiero, Unité d'Immunohématologie et d'Immunopathologie de l'Institut Pasteur, 28, rue du Docteur Roux, 75724 Paris cedex 15, France. Phone: (33) (1) 45 68 82 10; FAX: (33) (1) 45 68 89 51; E-mail: dighiero@pasteur.fr

Received for publication 29 April 1996 and accepted in revised form 11 September 1996.

1. *Abbreviations used in this paper:* CDR, complementary determining region; CNBr, cyanogen bromide; FR, framework region; LC/ESMS, liquid chromatography/electrospray mass spectrometry; R, replacement; S, silent.

J. Clin. Invest.

0021-9738/96/11/2235/09 $2.00
Volume 98, Number 10, November 1996, 2235–2243

starting buffer. The different peaks were analyzed by SDS-PAGE. $F(ab')_2$ fragments were obtained by digesting 3 mg of $IgG1\kappa^{PER}$ for 24 h at 37°C with 50 μg of pepsin in acetate buffer, pH 4.5, followed by a gel filtration chromathography (Superose 12 column; Pharmacia Fine Chemicals, Uppsala, Sweden).

To obtain purified Fabα fragments, 50 mg of monomeric $IgA1\kappa^{PER}$ were digested overnight at 37°C with 100 μg of IgA1-protease (Boehringer Mannheim, Mannheim, Germany) and subsequently purified by DEAE-Sepharose and gel filtration chromatography. $F(ab')_2$ fragments were obtained by digesting 10 mg of monomeric $IgA1\kappa^{PER}$ for 48 h at 37°C with a 100 μg pepsin solution in acetate buffer, pH 4.5, followed by a gel filtration chromatography (Superose 12 column).

Sample preparation for Edman degradation and mass spectrometry analyses

Ig heavy and light chain purification. Ig were denaturated in 6 M guanidine-HCl, 1 mM EDTA, 0.4 M Tris, pH 8.2, and reduced by incubating for 2 h at 37°C with 8 mM dithiothreitol. Cysteine residues were carboxymethylated with 20 mM iodoacetic acid for 1 h at 37°C followed by overnight at 4°C. Separation of heavy and light chains was performed by gel filtration through a Sephadex G-100 column in 1 M acetic acid and 8 M urea. The purified proteins were dialyzed against 0.5% acetic acid and lyophilized.

Cyanogen bromide cleavage. The reduced-alkylated heavy chains were dissolved in 70% trifluoroacetic acid. Cyanogen bromide (CNBr) was added to this solution (CNBr/protein = 50 wt/wt) and the reaction was allowed to proceed at 4°C for 20 h in the dark, and was terminated by addition of 10 vol water before lyophilization.

Enzymic digestion. Lysine endopeptidase digestion of reduced-alkylated entire light chains and of CNBr peptides of reduced-alkylated heavy chains was performed at 37°C in 100 mM Tris-HCl, pH 8.2, 1 mM EDTA, at an enzyme/substrate ratio of 1:50 (wt/wt). The IgG_1 light chain peptide P1-117 was obtained by reverse-phase HPLC of a low molecular weight fraction of the pepsin digest performed for F(ab′)2 preparation. Tryptic digestion of P1-117 was performed at 37°C in 100 mM Tris-HCl, pH 8.2, 5 mM $CaCl_2$ at an enzyme/substrate ratio of 1:50 (wt/wt). Lysis times (4–24 h) were adjusted by reverse-phase HPLC study of small aliquots during digestion.

Reverse phase HPLC. Separation of peptides generated by CNBr or enzymic cleavage was carried out using a system (130A; Applied Biosystems, Inc., Foster City, CA). The C8 column (Aquapore RP-300, 100 × 2.1 mm; Applied Biosystems, Inc.) was eluted with a linear gradient of 5–80% acetonitrile (0.1% trifluoroacetic acid) for 45 min at 200 μl/min.

Mass spectrometry

Liquid chromatography/electrospray mass spectrometry (LC/ESMS) was performed using a Sciex AP I/III triple quadrupole mass spectrometer (Perkin-Elmer Sciex Instruments, Thornhill, Canada) equipped with an atmospheric pressure ionisation source and a Sciex IonSpray interface. A Carlo Erba (Pheonix 20, Fisons Instruments Laboratory Systems, Altrincham, UK) liquid chromatograph, equipped with a homemade reverse-phase capillary column (Nucleosil C8, 0.25 × 150 mm, fused silica; Macherey Nagel, wDüren, Germany), was coupled directly to the mass spectrometer. Separation of digests were performed with a linear gradient of 5–80% acetonitrile (0.1% trifluoroacetic acid) in 60 min at a flow rate of 5 μl/min. The spectra were recorded in the 500–1,500 range of mass-to-charge ratio using dwell times of 2 ms.

Amino acid sequence determination

Automated Edman degradation was performed using a gas-phase Sequencer (477 A; Applied Biosystems, Inc.) with on-line analysis of the phenylthiohydantoin derivatives. Repetitive yields varied between 90 and 95%, depending on the peptide sequence.

V_H and V_L nucleotide sequence of $IgA1\kappa^{PER}$

cDNA preparation. RNA was isolated from 10^6 PBMC by the guanidinium thiocyanate-phenol-chloroform method (11). cDNA synthesis was performed in a 20-μl reaction volume at 37°C for 60 min using an oligo dT primer 15-mer (Boehringer Mannheim), 200 U of Moloney murine leukemia virus reverse transcriptase (GIBCO BRL, Bethesda, MD), 40 U of RNAse inhibitor (Boehringer Mannheim) and 0.5 mM of each deoxyribonucleotide.

V_H and V_L amplification by PCR. PCR amplification was carried out from 1 μg of single-stranded cDNA using *Taq* DNA polymerase (Perkin-Elmer Cetus Instruments, Emeryville, CA). According to the amino acid sequence the 5′ primer used for V_H gene amplification was designed to anneal to the leader region of the V_H3 family (5′ L_H3 fow: GTA TCG ATG GAG TTT GGG CTG AGC TGG), and an antisense oligonucleotide specific to C_H1 domain of Cα region was used as the 3′ primer (3′ Cα-rev: ATC TGG CTG GGT GCT GCA GAG GCT). The 5′ primer used for $V_\kappa II$ gene amplification was designed to anneal specifically to the framework 1 (FR1) region of this kappa light chain family (5′ V_κII-fow: CTA GAG TCG ACG ATA TTG TGA TGA CTC AGT CTC C), and in 3′, the consensus C_κ primer (3′ C_κ-rev: CAG ATG GCG GGA AGA TG) was used. In all cases, 30 cycles of amplification (95°C 1′, 62°C 1′, and 72°C 1′) were carried out.

V_H and V_L cloning and sequencing. Purified PCR fragments were ligated in blunt ends into the SmaI site of pBluescript KS+ phagemide vector. XL-1 blue *Escherichia coli* were transformed and selected in culture medium containing ampicillin. Recombinant plasmids were purified from transformed bacteria and selected by restriction analysis. Nucleotide sequencing was performed by the dideoxy chain termination method (Promega Corp., Madison, WI). All inserts were sequenced from two strands and from three independent clones. Nucleotide sequence data were analyzed and comparisons were carried out with the GCG software package and the GenBank/EMBL/DDBJ database.

Establishing germinal counterparts of H and L chains from $IgA1\kappa^{PER}$ and $IgG1\kappa^{PER}$

V_H3 (V_H germ) and $V_\kappa II$ (V_κ germ) germline nucleotide sequences obtained from autologous genomic DNA of the patient's T cells were compared to the 3-73 (clone MTGL) (12) and V_κIIA3 germline genes (13), and to the nucleotide sequence obtained from the cDNA of the patient's peripheral blood B cells expressing $IgA1\kappa^{PER}$. T cells from the patient's PBMC were cultured for 4 wk in the presence of PHA plus IL-2. Genomic DNA was extracted from T lymphocytes of the patient and nonrearranged V_H3 genes were amplified with the same consensus 5′ L_H3 fow and an antisense heptamer-spacer 3′ primer (V_H3-rev: CAC AGT GAG GGG AGG TCA GTG TGG TCG ACC T). The amplified products were cloned and sequenced as described (11). Identification of the germline counterpart was achieved using a specific CDR2 probe (ACG CGA CAG CAT ATG CTG CGT CG). $V_\kappa II$ nonrearranged genes were amplified using the same consensus 5′ $V_\kappa II$ family primer and a 3′ $V_\kappa II$ heptamer-spacer-nonamer reverse primer (V_κII-rev: GTA TCG ATG TTT CTG TTA GGG GTT GTA CCA CTG TG). Amplified fragments were cloned, selected by a specific reverse 3′V_κII-FR3 probe (TGT AAA ATC TGT GCC TGA TCC ACT) and sequenced.

Affinity and kinetic constants determination by surface plasmon resonance (14)

Equilibrium and kinetic constants for the interactions between MIg and tubulin were determined by the BIAcore™ system (Pharmacia Biosensor AB, Uppsala, Sweden). Immobilization of tubulin via primary amines to the Sensorchip CM5 was performed using amine coupling kit (Pharmacia Biosensor AB). Activation of the carboxymethylated dextran matrix was obtained by injecting a mixture of *N*-ethyl-*N*′-(dimethylaminopropyl) carbodiimide and *N*-hydroxysuccinimide.

Tubulin was prepared at a concentration of 25 μg/ml in 100 μl of a 10 mM acetate buffer, pH 4.1. Deactivation of remaining esters was obtained by injecting a solution of ethanolamine-HCl. In all runs, PBS was used as driving eluent. 100 μl of different mAb fractions at the following concentrations: $IgA1\kappa^{PER}$, 135, 13.5, and 1.35 nM;

Table I. Equilibrium and Kinetic Constants for MIg^{PER} Binding to Tubulin

	k_{DISS} (s^{-1})	k_{ASS} ($M^{-1}\,s^{-1}$)	K_D (M)
IgA1κ^{PER}	4.19×10^{-4}	1.47×10^{4}	2.85×10^{-8}
F(ab′)2 IgA1κ^{PER}	4.64×10^{-4}	1.41×10^{4}	3.29×10^{-8}
Fab IgA1κ^{PER}	7.01×10^{-4}	1.16×10^{4}	6.04×10^{-8}
IgG1κ^{PER}	1.59×10^{-3}	1.56×10^{3}	1.02×10^{-6}
F(ab′)2 IgG1κ^{PER}	1.51×10^{-3}	*	—
Fab IgG1κ^{PER}	2.20×10^{-3}	*	—

Affinity and kinetic constants determination by surface plasmon resonance. *Association rate constants for IgG1κ^{PER} F(ab′)2 and Fab fragments were too slow and thus could not be calculated.

IgG1κ^{PER}, 10 and 2.5 μM, and 500 and 100 nM; F(ab′)2 and Fab IgA1κ^{PER}, 1 μM and 100 nM; F(ab′)2 and Fab IgG1κ^{PER}, 2.3 and 1 μM were allowed to bind to immobilized tubulin at a flow of 5 μl/min, and binding events as well as the dissociation in buffer flow were recorded in sensorgrams at 20°C. The amount of Ab bound (R_{max}) to the tubulin as well as the reaction rate (dR/dt) were calculated using the Bialogue™ software. Kinetic rate constants (k_{ASS} and k_{DISS}) as well as apparent equilibrium affinity constants ($K_D = k_{DISS}/k_{ASS}$) were determined using Bialogue™ Kinetics Evaluation software (Table I). Background binding was determined by analyzing the sensorgram of the dextran surface–MIg interaction. Surface reconstitution was performed by eluting with a 1 M NaCl solution.

To investigate the role of temperature on association and dissociation of IgA1κ^{PER} with tubulin, binding assays in the same above described conditions were carried out at 15, 20, 28, 31, and 37°C.

Measurement of the affinity constant in solution by ELISA (15)

Various concentrations of tubulin were individually incubated in solution with IgA1κ^{PER} and IgG1κ^{PER} at constant concentration until equilibrium was reached (15 h at 20°C). The concentration of free Ab was then measured by an indirect ELISA after incubating at 20°C for 15 min (incubation time was determined to avoid equilibrium displacement). The correlation between enzymatic activity and the concentration of free Ab in solution was first established by adding various known amounts of Ab in coated wells, under experimental conditions identical to those used in the binding experiment. This calibration allows the determination of the free Ab concentration at

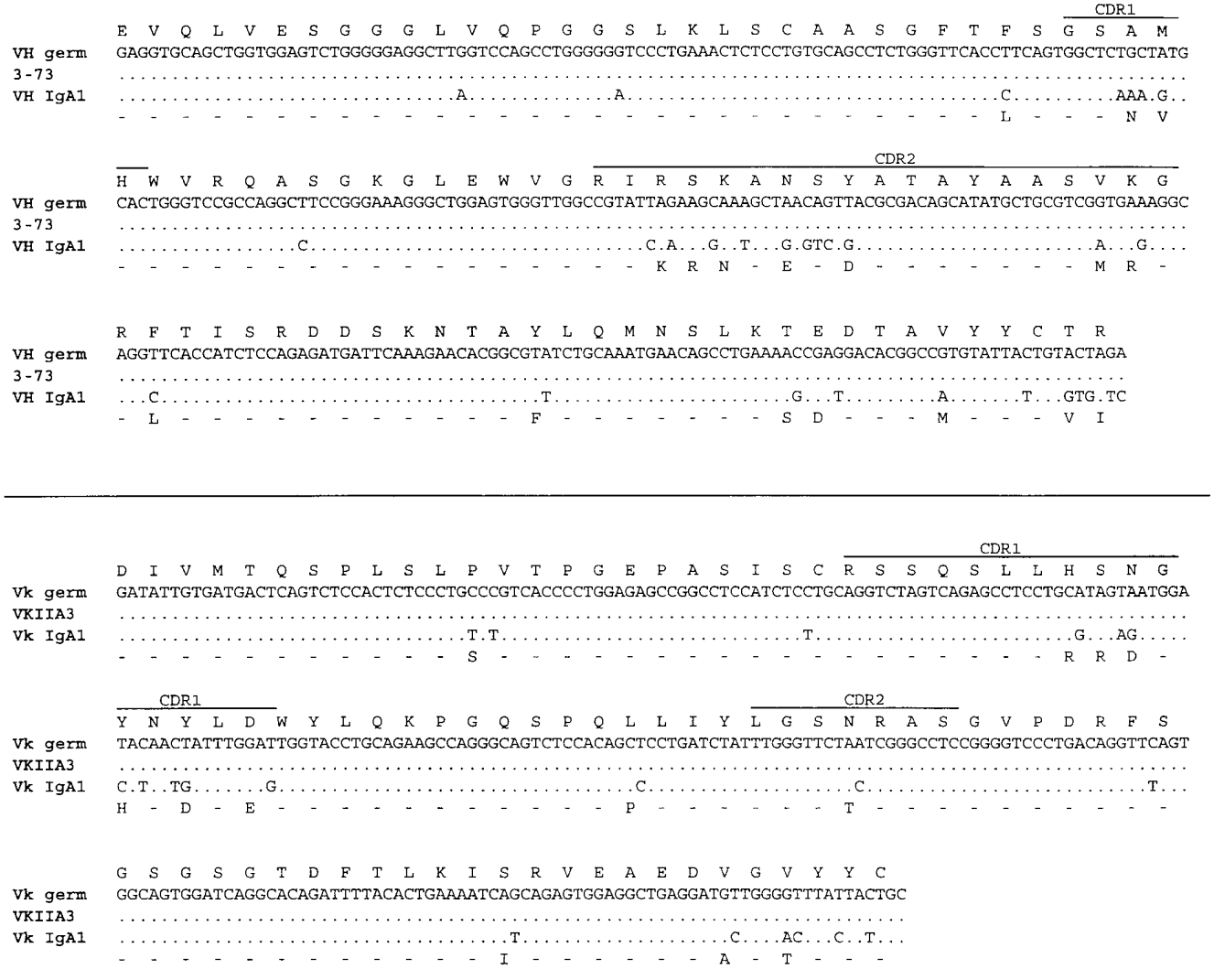

Figure 1. Determination of V_H and V_L nucleotide sequence and germline counterpart of IgA1κ^{PER}. Amino acid and nucleotide sequences of V_H and V_L segments from IgA1κ^{PER} and their germinal V_H and V_L counterparts (V_H and V_κ *germ*), compared with the most closely matching germline genes (*3-73* and *VKIIA3*). Nucleotide sequence and amino acid identity are respectively indicated by dots and dashes. Replacements are depicted by bottom case letters. CDR1 and CDR2 domains are indicated.

equilibrium, provided that the total Ab concentration is known. The affinity constant was determined by Scatchard plot analysis.

Results

Determination of V_H and V_L nucleotide sequence and germline counterpart of IgA1κ^{PER}. In agreement with cytometric results showing that almost all peripheral blood cells from patient PER were expressing IgAκ (10), PCR amplification products could only be obtained for this MIg. In a first step, the cDNA nucleotide sequences encoding the heavy and light chain V domains of IgA1κ^{PER} were determined. This MIg expressed a V_H3 family member gene (Fig. 1) associated to a DXP′1 D segment and to a JH4 segment (Fig. 2) and a $V_κ$II family member gene rearranged to a $J_κ$5 (Figs. 1 and 2).

To evaluate the importance of the somatic mutation process in the generation of these autoantibodies and to avoid misinterpretation related to V gene polymorphisms, we have determined the V_H and V_L germline counterparts of the MIgs.

Fig. 1 shows the germline nucleotide V_H and V_L sequences obtained from autologous T cell genomic DNA. By parsimony, it was determined that the H chain variable domain most likely derived from the V_H3 gene segment 3–73 (12), and the L chain variable domain from the $V_κ$II A3 gene segment (reference 13 and Fig. 1). In the heavy chain, there were eight and four codons that respectively underwent replacement (R) and silent (S) mutations in the frameworks (R:S ratio of 2), and there were nine replacement and three silent mutations in CDRs 1 and 2 (R:S ratio of 3). Similarly, in the light chain, there were five and four codons that respectively underwent replacement and silent mutations in the frameworks (R:S ratio of 1.25), and there were seven replacement mutations and only one silent mutation in CDRs 1 and 2 (R:S ratio of 7.0). Mutations and replacements predominated in CDR of both H and L chains and induced a significant hydrophobicity shift in these domains (data not shown). Interestingly, in the middle of the H chain CDR2 occurs an unmutated region displaying a palindromic sequence (CAGCATATGCTG) with a potential stem-loop structure. Similar structures have been found in other V region genes and could act as entry sites for a repair mechanism favoring local mutation (16).

Somatic mutations resulting in multiple replacement mutations in the CDRs with preservation of the peptide sequence of the frameworks are typical of Abs that have undergone selection by Ag. In addition, mutations in FRs predominated in the FR3 domain of both H and L chains, a region that may itself contribute to Ag recognition (17).

Amino acid sequence of the IgG1κ^{PER} light chain. Comparison with the IgA1κ^{PER} light chain sequence. IgG1κ^{PER} and IgA1κ^{PER} light chains were prepared in the carboxymethylated form by Sephadex G-100 gel filtration (not shown). Their lysine endopeptidase digests were compared by reverse-phase HPLC. Interestingly, the two chromatographic profiles (Fig. 3) showed identical retention times for all the peptides. Sequencing of the separated lysine endopeptidase peptides of the IgG1^{PER} light chain was performed and permitted the determination of about 80% of the aminoacids (Fig. 4).

A peptide (P1-117) was isolated from a pepsin digest of the unreduced IgG1κ^{PER} molecule and subdigested with trypsin before separation by reverse-phase HPLC (not shown). Edman degradation of the purified peptides of P1-117 permitted the completion of the amino acid sequence of the variable region (Fig. 4).

Finally, except for residues 189–195 and 213–219 (underlined in Fig. 4 and taken from Kabat et al., reference 1) of the constant region, the almost complete amino acid sequence of the IgG1κ^{PER} light chain was determined by Edman degradation. The NH_2-terminal part of this sequence, including all the variable domain, showed a perfect identity with the determined part of the IgA1κ^{PER} light chain (Figs. 1, 2, and 4). In addition, NH_2-terminal amino acid sequencing of IgA1κ^{PER} light chain was performed (data not shown). The determined sequence (residues 1–24) covered the region corresponding to the FR1 primer (residues 1–8) and was identical to the deduced sequence.

Mass spectrometry analyses (LC/ESMS) of the carboxymethylated entire IgG1κ^{PER} and IgA1κ^{PER} light chains, of their lysine endopeptidase digests, and of the tryptic digest of IgG1-117, were performed. The expected mass of the carboxymethylated IgG1 light chain, calculated from its amino acid sequence, is 24,275.0 D. The measured masses of the IgG1κ^{PER} and IgA1κ^{PER} carboxymethylated light chains are 24,272±5 and 24,271±5D, respectively (not shown). The measured mass of all the peptides issued from the IgG1κ^{PER} light chain digests corresponded well with their expected masses (Fig. 4). Finally, the measured masses (not shown) of the peptides issued from the lysine endopeptidase digest of the IgA1κ^{PER} light chain corresponded exactly with the masses of the corresponding

VH germline //Y Y C T R //TATTACTGTACTAGA //.....T...GTG.TC //- - - V I **VH-FR3 IgA1 end**	**DXP′1** **JH4 germline** R G V I Y F D Y CGGGGAGTTATT TACTTTGACTAC .......A.G.. ...AACCGAC.G - - D V - N R Q **VH-CDR3 IgA1**	**JH4 germline** W G Q G T L V T V S S TGGGGCCAGGGAACCCTGGTCACCGTCTCCTCA .... - - - - - - - - - - - **VH-FR4 IgA1**	**CH1 alpha germline** A S P T S P K V F P L primer Cα rev GCATCCCCGACCAGCCCCAAGGTCTTCCCGCTGAGCCTCTGCAGCACCCAGCCAGAT// ....agcctctgcagcacccagccagat// - - - - - - - - - - - - - - - - - - - // **CH1 IgA1**
Vκ germline G V Y Y C //GGGGTTTATTACTGC //...AC...C..T... //- T - - - **Vκ-FR3 IgA1 end**	**Vκ germline** **Jκ5** M Q G L Q T P I T ATGCAAGCTCTACAAACTCCT ATCACC ......AA.AA.........C C..... - - N K - - - L - **Vκ-CDR3 IgA1**	**Jκ5 germline** F G Q G T R L E I K TTCGGCCAAGGGACACGACTGGAGATTAAA .... - - - - - - - - - - **Vκ-FR4 IgA1**	**Cκ germline** R T V A A P S V F primer Cκ rev CGAACTGTGGCTGCACCATCTGTCTTCATCTTCCCGCCATCTG// ....catcttcccgccatctg// - - - - - - - - - - - - - - // **Cκ IgA1**

Figure 2. CDR3 and FR4 regions from IgA1κ^{PER} H and L chains. Amino acid and nucleotide sequence of H and L CDR3 regions are compared with the closest germinal counterpart. Replacements are depicted by bottom case letters. $C_α$ and $C_κ$ reverse primers are indicated by lower case letters.

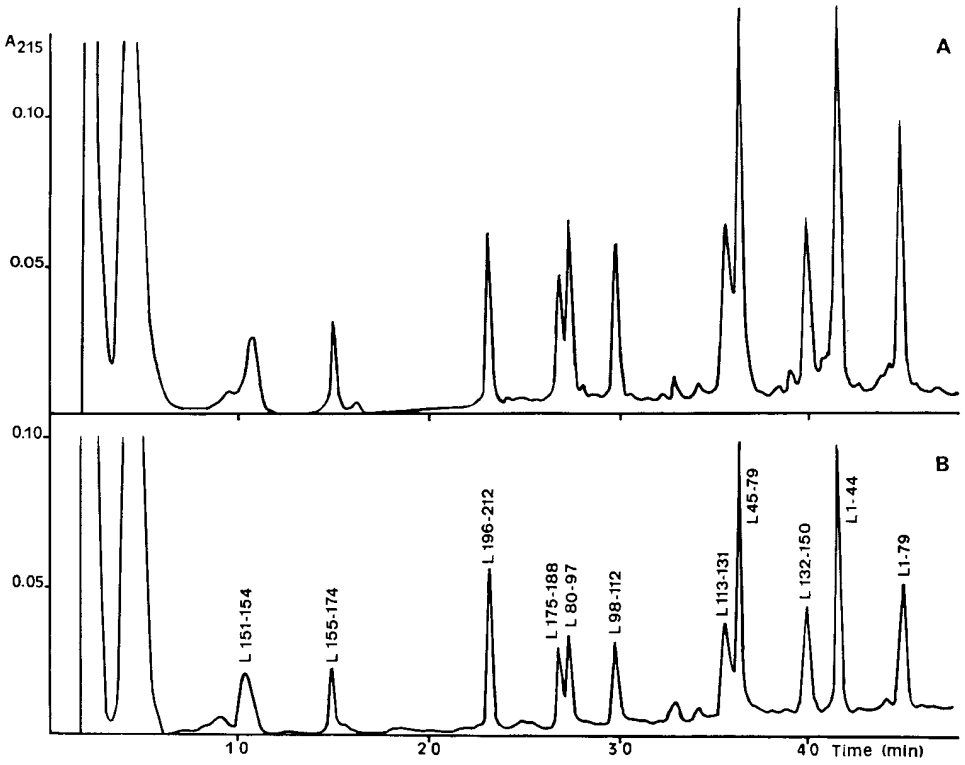

Figure 3. Reverse phase HPLC separation of peptides generated by lysine endopeptidase digestion. (*A*) IgA1κ^{PER} and (*B*) IgG1κ^{PER} light carboxymethylated chains. The peptides (Lx-x) were identified by Edman degradation and mass spectrometry (see Fig. 4).

peptides issued from the IgG1κ^{PER} light chain. Mass spectroscopy analyses excluded the possibility of amino acid insertions in the junctions between identified peptides.

Hence, these results unambiguously prove the complete identity of the IgG1κ^{PER} and IgA1κ^{PER} kappa light chains.

Amino acid sequence of the NH_2-terminal part of the IgG1κ^{PER} heavy chain. Comparison with the IgA1κ^{PER} heavy chain sequence. Carboxymethylated IgG1κ^{PER} and IgA1κ^{PER} heavy chains purified by Sephadex G-100 gel filtration were submitted to CNBr cleavage and reverse-phase HPLC (not shown). The chromatographic profiles of the two digests were different except for a few fractions. Compared mass spectrometry (LC/ESMS) analysis of the two heavy chain digests showed identity of the measured masses for three well defined peptides, showing identical retention times (data not shown). The three peptides isolated by HPLC chromatography of the IgG1κ^{PER} digest were submitted to Edman degradation. These studies permitted determination of the partial or complete sequence of these three socalled peptides CB1-66, CB67-85, and CB67-95. The NH_2-terminal sequence of a high mass peptide (CB96. . .) was also established (Fig. 5). All these determined amino acid sequences of the IgG1κ^{PER} heavy chain corresponded exactly with sequences of the variable region of the IgA1κ^{PER} heavy chain (Figs. 1 and 2).

Peptide CB1-66, and higher mass fractions of the IgG1 heavy chain CNBr digest, were submitted to lysine endopeptidase cleavage, Edman degradation, and mass spectrometry analyses. A set of peptides permitted to define the complete sequence of the variable region (amino acids 1–119) and to determine a large part of the CH1 constant domain (Fig. 5). The peptides L90-123, L150-207, and L150-212 were only partially sequenced, but their measured masses corresponded well with their expected masses deduced from partial sequencing and from the data of Kabat et al. (1). Mass spectroscopy analyses excluded the possibility of amino acid insertions in the junctions between identified peptides. The mass of the so called peptides CB96. . .could not be measured, but its NH_2-terminal sequence (amino acids 96–120) was confirmed and completed by analysis of smaller peptides.

Overall, comparison of the complete IgG1κ^{PER} heavy chain NH_2-terminal sequence (Fig. 5) with the corresponding IgA1κ^{PER} heavy chain sequence (Figs. 1 and 2) proves the complete identity of the variable regions and shows the expected differences in the CH1 constant domain.

In a previous work (10), a difference was reported in position 6 of the NH_2-terminal amino acid sequence of the heavy of the four clonally related MIg, including the two compared in this work. Careful reexamination (data not shown) of these NH_2-terminal sequences was performed and unambiguously showed that the amino acid residue in position 6 was always a glutamic acid (*E*) and never a glutamine (*Q*).

Affinity and kinetic constant determination against tubulin for IgA1κ^{PER} and IgG1κ^{PER}. In a previous study, both MIg^{PER} were found to bind tubulin (10), even after dissociation and cross-reassociation of H and L chains. In addition, after limited enzymatic proteolysis of tubulin, both MIg^{PER} were shown to recognize overlapping epitopes in the carboxy-terminal region of both α and β tubulin subunits, with minor differences in the specificity. However, in spite of sharing identical variable domain sequences, having identical light chain constant domains and recognizing overlapping epitopes on the Ag, both Ab significantly differed in the K_D for tubulin as determined by measuring surface plasmon resonance (2.85×10^{-8} M for IgA1κ^{PER} and 1.02×10^{-6} M for IgG1κ^{PER}) (Table I) or by Friguet's assay (6.9×10^{-9} M for IgA1κ^{PER} and 5.0×10^{-6} M for IgG1κ^{PER}). To determine whether these differences were due

```
         10         20         30         40         50         60
DIVMTQSPLSLSVTPGEPASISBRSSQSLLRRDGHNDLEWYLQKPGQSPQPLIYLGSTRA
         70         80         90        100        110        120
SGVPDRFSGSGSGTDFTLKIIRVEAEDAGTYYBMQNKQTPLTFGQGTRLEIKRTVAAPSV
        130        140        150        160        170        180
FIFPPSDEQLKSGTASVVBLLNNFYPREAKVQWKVDNALQSGNSQESVTEQDSKDSTYSL
        190        200        210
SSTLTLSKADYEKHKVYABEVTHQGLSSPVTKSFNRGEB
```

Fragment	Sequence (Edman degradation)	Expected mass(Da)	Measured mass(Da)
L1-44	DIVMTQSPLSLSVTPGEPASISBR---	inc.seq.	4974.0
L45-79	PGQSPQPLIYLGSTRASGVPDRFSGS---	inc.seq.	3582.0
L80-97	IIRVEAEDAGTYYBMQNK	2162.44	2162.5
L98-112	QTPLTFGQGTRLEIK	1688.96	1689.0
L113-131	RTVAAPSVFIFPPSDEQLK	2102.43	2102.0
L132-150	SGTASVVBLLNNFYPREAK	2127.41	2128.2
L151-154	VQWK	559.68	559.5
L155-174	VDNALQSGNSQESVTEQDSK	2136.18	2136.0
L175-188	DSTYSLSSTLTLSK	1502.65	1502.2
L196-212	VYABEVTHQGLSSPVTK	1877.11	1876.8
P1-117	DIVMTQSPLSLSVTPGEPA---	inc.seq.	12735.0
T1- 24	DIVMTQSPLSLSVTPGEPASISCR		
|	|	4591.28	4591.2
T80-97	IIRVEAEDAGTYYCMQNK		
T1- 24	DIVMTQSPLSLSVTPGEPASISCR		
|	|	4208.78	4208.4
T83-97	VEAEDAGTYYCMQNK		
T25-31	SSQSLLR	789.90	789.5
T25-32	SSQSLLRR	946.08	n.obs.
T32-59	RDGHNDLEWYLQKPGQSPQPLIYLGSTR	3269.64	3269.4
T33-59	DGHNDLEWYLQKPGQSPQPLIYLGSTR	3113.45	3113.1
T60-79	ASGVPDRFSGSGSGTDFTLK	1986.13	1985.5
T67-79	FSGSGSGTDFTLK	1303.40	1302.0
T98-108	QTPLTFGQGTR	1205.35	1205.0
T109-112	LEIK	501.63	n.obs.
T109-113	LEIKR	657.82	657.5

Figure 4. Amino acid sequence of the IgG1κ^{PER} light chain determined by Edman degradation and mass analyses (LC/ESMS). Lx-x, lysine endopeptidase peptides obtained from the reduced-alkylated entire light chain; B, carboxymethylated cysteine; P1-117, NH_2-terminal peptide of the light chain purified from a pepsin digest of the unreduced IgG1 molecule; Tx-x, tryptic peptides derived from P1-117; inc. seq., incompletely sequenced peptide; n. obs., nonobserved peptide. Underlined amino acid residues 189–195 and 213–219 have not been determined in this work and are from Kabat et al. (1). The expected masses of peptides L1-44, L45-79, and P1-117 could be calculated after analysis of the tryptic digest and are 4,974.57, 3,581.96, and 12,734.34 D, respectively.

to interactions between the Fc portions of the Ab, F(ab′)2 and Fab fragments were prepared (Fig. 6). The relative differences in the affinity constants between IgG1κ^{PER} and IgA1κ^{PER} were preserved at the Fab level (Table I). These values were of 3.29×10^{-8} M for F(ab′)2 and 6.04×10^{-8} M for Fab from IgA1κ^{PER}, but could not be calculated for IgG1κ^{PER} fragments since association rates were too slow to be measured, even after running the sample for 120 min. To obtain measurable K_D in these conditions would require an exposition time of several hours (18). Thus, this difference in affinity could be attributed to the C_H1 domain.

Kinetic analysis demonstrated that this difference in affinity was mainly accounted for by a disparity in the association rate constants (1.47×10^4 M^{-1} s^{-1} for IgA1κ^{PER} and 1.56×10^3 M^{-1} s^{-1} for IgG1κ^{PER}), with only slight differences in the dissociation rate constants (4.19×10^{-4} s^{-1} for IgA1κ^{PER} and 1.59×10^{-3} s^{-1} for IgG1κ^{PER}, Table I). The differences in the association rate constants would suggest however, that the pathway leading to the formation of a stable complex might differ. We analyzed the effect of changing the temperature on complex formation of IgA1κ^{PER} and tubulin (Table II and Fig. 7). The amount of Ab bound at equilibrium decreased with increasing temperature from 15 to 37°C. Although the dissociation rate steadily increased across this temperature range, the association rate decreased. In addition, similar results were observed with the Fab fragment from IgA, where the association constant at 37°C was 5.72×10^3 M^{-1} s^{-1} as compared with 1.16×10^4 M^{-1} s^{-1} at 20°C and the dissociation rate constants of 7.89×10^{-3} s^{-1} (7.01×10^{-4} s^{-1} at 20°C). Similar changes were observed in the association process for Fab and complete IgA. However, a more rapid dissociation could be observed for the monovalent Fab. It remains unclear whether these differences could be related to the bivalency of the complete IgA.

Discussion

Our results show that two different Igs unambiguously sharing identical V_H and V_L domains, but expressing different heavy constant regions bind tubulin with significant differences in affinity. The observation that even Fab fragments from these Ab reproduce differences in binding suggests that structural differences in the C_H1 domain underlie the differences in the affinity constants, and thus the differences in Ag binding.

As for affinity studies, a number of data are now available

```
         10         20         30         40         50         60
EVQLVESGGGLVQPGGSLKLSBAASGFTLSGSNVHWVRQASGKGLEWVGRIKRNAESDAT
         70         80         90        100        110        120
AYAASMRGRLTISRDDSKNTAFLQMNSLKSDDTAMYYBVIRGDVYNRQWGQGTLVTVSSA
        130        140        150        160        170        180
STKGPSVFPLAPSSKSTSGGTAALGBLVKDYFPEPVTVSWNSGALTSGVHTFPAVLQSSG
        190        200        210
LYSLSSVVTVPSSSLGTQTYIBNVNHKPSNTK
```

Fragment	Sequence (Edman degradation)	Expected mass(Da)	Measured mass(Da)
CB1-66	EVQLVESGGGLVQPGGSLKLSBAASGFTL---	inc.seq.	6788.0
CB67-85	RGRLTISRDDSKNTAFLQm'	2161.42	2161.0
CB67-95	RGRLTISRDDSKNTAFLQ(MO)NSLKSDDTAm'	3240.58	3240.0
CB96...	YYBVIRGDVYNRQWGQGTLVTVSSA---	inc.seq.	n.obs.
L1-19	EVQLVESGGGLVQPGGSLK	1854.10	1854.0
L20-43	LSBAASGFTLSGSNVHWVRQASGK	2521.80	2521.5
L44-52	GLEWVGRIK	1057.27	1057.0
L53-78	RNAESDATAYAAS(MO)RGRLTISRDDSK	2859.10	2859.0
L79-89	NTAFLQ(MO)NSLK	1282.49	1282.0
L90-123	SDDTA(MO)YYBVIRGDVYNRQWGQGTLVTV---	3847.22*	3847.0
L124-135	GPSVFPLAPSSK	1186.38	1186.0
L136-149	STSGGTAALGBLVK	1322.51	1322.0
L150-207	DYFPEPVTVSWNSGALTSGVHTFPAVLQ---	6189.88*	6190.0
L150-212	DYFPEPVTVSWNSGALTSGVHTFPAVLQ---	6717.45*	6717.0

Figure 5. Amino acid sequence of the NH_2-terminal region of the IgG1κ^{PER} heavy chain determined by Edman degradation and mass analyses (LC/ESMS). CBx-x, CNBr peptides obtained from the reduced-alkylated heavy chain; Lx-x, lysine endopeptidase peptides obtained by digestion of CNBr peptides; m′, homoserine lactone; (MO), methionine sulfoxide; B, carboxymethylated cysteine; inc. seq., incompletely sequenced peptide; n. obs., nonobserved peptide. Underlined amino acid residues 121–123 and 178–212 have not been determined in this work and are from Kabat et al. (1). *Expected masses calculated from the sequences partially determined by Edman degradation and completed by the data from Kabat et al. (1). The expected mass of peptides CB1-66 could be calculated after analysis of the lysine endopeptidase digest and is 6,788.55 D.

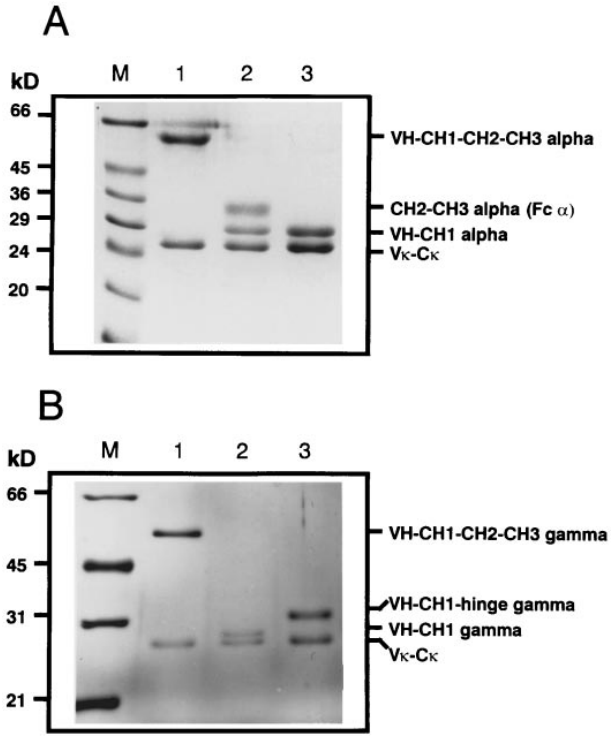

Figure 6. SDS-PAGE of reduced purified Ig and Fab fragments from IgA1κ^{PER} and IgG1κ^{PER}. (*A*) Lane *1*, monomeric IgA1κ^{PER}; lane *2*, after digestion with IgA1 protease; and lane *3*, purified Fab after ion-exchange chromatography. (*B*) Lane *1*, IgG1κ^{PER}; lane *2*, purified Fab; and lane *3*, purified (Fab′)2.

on kinetic measurements of antigen-antibody interactions assessed by surface plasmon resonance (8, 19–22). These studies show that equilibrium constants of these interactions vary from 10^6 to 10^{11} with k_{ass} values ranging from 10^3 to 10^6 and k_{diss} ranging from 10^{-3} to 10^{-5}. Our results for IgA1κ^{PER}-tubulin binding are consistent with a conventional Ag–Ab interaction.

In a previous work (23), we studied 135 different IgA MIgs. The pattern of binding to tubulin of this particular IgA1κ^{PER} was unique, thus excluding the possibility that the interaction between Ag and Ab occurred via a particular interaction between a C_H1 domain and tubulin or via a superantigen-like mechanism.

The smooth temperature profile of the dissociation rates for IgA suggests that dissociation is occurring from the same stable complex within the temperature range studied. In con-

Table II. Equilibrium and Kinetic Constants for IgA1κ^{PER} Binding to Tubulin as a Function of Temperature

	k_{DISS} (s^{-1})	k_{ASS} ($M^{-1}\,s^{-1}$)	K_D (M)
15°C	3.94×10^{-4}	1.70×10^4	2.32×10^{-8}
20°C	4.19×10^{-4}	1.47×10^4	2.85×10^{-8}
28°C	4.51×10^{-4}	1.25×10^4	3.61×10^{-8}
31°C	3.94×10^{-4}	1.31×10^4	3.01×10^{-8}
37°C	7.84×10^{-4}	6.01×10^3	1.30×10^{-7}

Temperature dependence of IgA1κ^{PER} binding constants. Affinity measurements were carried out at 15, 20, 28, 31, and 37°C. Dissociation rates increase with increasing temperature, whereas the reverse occurs for association rate constants.

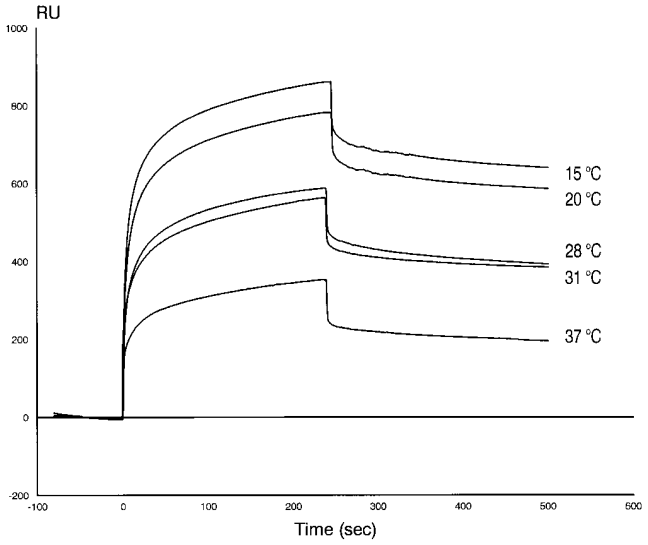

Figure 7. Role of temperature on association and dissociation of IgAκ^{PER} with tubulin. Sensorgrams obtained with IgAκ^{PER}, when kinetic measurements were carried out at 15, 20, 28, 31, and 37°C. Results are expressed as Resonance units (*RU*) as a time (sec) function.

trast, there is an unusual change seen in the association rate as a function of temperature. At 37°C there is weak discrimination in favor of the stable complex, whereas at low temperature a stable complex is favored. There is a change in a rate-limiting step on a sequential pathway leading to this stable complex. Differences in the C_H1 domain could lead to the formation of different structural isomers that attenuate the rates at which the variable domains undergo the necessary conformational changes required for formation of a stable Ag–Ab complex. No measurable changes in the weak association rates for IgG1κ^{PER} with tubulin as a function of temperature could be obtained. This suggests that at high temperature the IgA1κ^{PER}-tubulin reaction approaches IgG1κ^{PER}-tubulin reaction and that the formation of the final stable complex in both cases may be impeded by some conformational rearrangement subsequent to initial binding. Thus, these results suggest that the same antigen-binding site displays different specificities when juxtaposed with different heavy chains. This could explain the differences in binding of these two MIg (discrete polyreactive binding including tubulin for IgG1κ^{PER}, exclusive binding to tubulin for IgA1κ^{PER}) (10).

It has long been assumed that the constant domains do not play a role in the maturation of Ag–Ab interactions. Indeed, Fabs are pseudosymetric dimers where V_H contacts with C_H1, whereas no contact is observed between V_L and C_L (24). Although crystallographic studies have shown that amino acids ensuring the link between Fv and C_H1 and C_L are flexible and allow spatial arrangements facilitating binding of epitopes by Fabs, there is controversy concerning the possiblity that elbow bending could facilitate signal transduction from the Ag-binding site to the Fc domain (25–28). However, recent work has demonstrated that changes in the C_H domains can affect the functional affinity and specificity of Abs, through a complex mechanism involving Ab flexibility and cooperative interactions in the case of Abs bound to multivalent Ags (8, 9). Schneider et al. (29) showed that segmental flexibility is controlled by the C_H1 domain and hinge regions of Abs, and Horgan et al. (30) reported that removal of the hinge region of an IgG4 resulted in a gain of relative affinity that approximated that observed with the same Ab expressing an IgG1 isotype. As concerns functional activity of Abs, Cavacini et al. (31) found that Ab isotype can strongly influence virion neutralization of the HIV-1 virus. Although the association of C_L and C_H1 necessarily increases the reach of the Ab and the probability of an appropriate quaternary interaction between V_L and V_H (32, 33), Bhat et al. (34) demonstrated that Fv and Fab fragments make very similar contacts with the Ag. However, Eigenbrot et al. (35) found contact differences in Fv and Fab fragments from the same Ab and Takahashi et al. (36) have shown that constant domains can affect the fluctuation of V_L domain. One difficulty in substantiating this by standard crystallography may arise from the fact that the role of molecular mobile components in the interaction with another molecule may not be fully captured by this method (27). This may emphasize the importance of kinetic studies on the elucidation of structural problems by allowing us to study the nature of transitions characterizing the formation of a physiologically relevant interaction (37).

It is presently unclear whether this observation could refer to an unusual mechanism and further work in different established Ag–Ab systems is warranted to establish how often this mechanism is employed by the immune system. Whatever the frequency with which this phenomenon could occur, these results favor the view that affinity maturation of this particular tumoral clone could be achieved through class switching in the absence of further somatic mutations, probably because the C_H1 domain plays a role in structuring the Ag-binding site into a more kinetically competent form.

Acknowledgments

We thank our colleagues P. Alzari, H. Buc, and A. Coutinho from the Pasteur Institute, R. Poljak (CARB, University of Maryland, Rockville, MD) and H.W. Schroeder (University of Alabama at Birmingham, Birmingham, AL) who kindly agreed to review this manuscript, and Mrs. Reine Bouyssié for secretarial assistance.

O. Pritsch is the recipient of a Grant from the Ministère de la Santé.

References

1. Kabat, E.A., T.T. Wu, M. Reid-Miller, H.M. Perry, and K.S. Gottesman. 1991. Sequences of Proteins of Immunological Interest. U.S. Government Printing Office, Bethesda, MD.

2. Tonegawa, S. 1983. Somatic generation of antibody diversity. *Nature (Lond.).* 302:575–581.

3. Yancopouylos, G.D., and F.W. Alt. 1986. Regulation of the assembly and expression of variable-region genes. *Ann. Rev. Immunol.* 4:339–368.

4. Kirkham, P.M., and H.W. Schroeder, Jr. 1994. Antibody structure and the evolution of immunoglobulin V gene segments. *Semin. Immunol.* 6:347–360.

5. Cebra, J.J., J.L. Komisar, and P.A. Schweitzer. 1984. CH isotype 'switching' during normal B-lymphocyte development. *Ann. Rev. Immunol.* 2:493–548.

6. Griffiths, G.M., C. Berek, M. Kaartinen, and C. Milstein. 1984. Somatic mutation and the maturation of immune response to 2-phenyl oxazolone. *Nature (Lond.).* 312:271–275.

7. Weigert, M., and R. Riblet. 1977. Genetic control of antibody variable regions. *Cold Spring Harbor Symp. Quant. Biol.* 41:837–846.

8. Cooper, L.J.N., D. Robertson, R. Granzow, and N.S. Greenspan. 1994. Variable domain-identical antibodies exhibit IgG subclass-related differences in affinity and kinetic constants as determined by surface plasmon resonance. *Mol. Immunol.* 31:577–584.

9. Cooper, L.J.N., A.R. Shikman, D.D. Glass, D. Kangisser, M.W. Cunningham, and N.S. Greenspan. 1993. Role of heavy chain constant domains in antibody-antigen interactions: apparent specificity difference among streptococcal

IgG antibodies expressing identical variable domains. *J. Immunol.* 150:2231–2242.

10. Houdayer, M., J.P. Bouvet, A. Wolff, C. Magnac, J.C. Guillemot, L. Borche, and G. Dighiero. 1993. Simultaneous presence, in one serum, of four monoclonal antibodies that might correspond to different steps in a clonal evolution from polyreactive to monoreactive antibodies. *J. Immunol.* 150:311–319.

11. Sambrook, J., E.F. Fritsch, and T. Maniatis. 1989. Molecular Cloning: A Laboratory Manual. Cold Spring Harbor Laboratory Press, New York.

12. Zelenetz, A.D., T.T. Chen, and R. Levy. 1992. Clonal expansion in follicular lymphoma occurs subsequent to antigenic selection. *J. Exp. Med.* 176: 1137–1148.

13. Straubinger, B., E. Huber, W. Lorenz, E. Osterholzer, W. Pargent, M. Pech, H.D. Pohlenz, F.J. Zimmer, and H.G. Zachau. 1988. The human VK locus. Characterization of a duplicated region encoding 28 different immunoglobulin genes. *J. Mol. Biol.* 199:23–34.

14. Malmqvist, M. 1993. Biospecific interaction analysis using biosensor technology. *Nature (Lond.).* 361:186–187.

15. Friguet, B., A.F. Chaffotte, L. Djavadi-Ohaniance, and M.E. Goldberg. 1985. Measurements of the true affinity constant in solution of antigen-antibody complexes by enzyme-linked immunosorbent assay. *J. Immunol. Methods.* 77:305–319.

16. Betz, A.G., C. Rada, R. Pannell, C. Milstein, and M.S. Neuberger. 1993. Passenger transgenes reveal intrinsic specificity of the antibody hypermutation mechanism: clustering, polarity, and specific hot spots. *Proc. Nat. Acad. Sci. USA.* 90:2385–2388.

17. Kehoe, J.M., and J.D. Capra. 1971. Localization of two additional hypervariable regions in immunoglobulin heavy chains. *Proc. Natl. Acad. Sci. USA.* 68:2019–2021.

18. BIAcore System Manual. 1991. Pharmacia Biosensor, Uppsala, Sweden.

19. Zeder-Lutz, G., D. Altschuh, H.M. Geysen, E. Trifilieff, G. Sommermeyer, and M.H.V. Van Regenmortel. 1993. Monoclonal antipeptide antibodies: affinity and kinetic rate constants measured for the peptide and the cognate protein using a biosensor technology. *Mol. Immunol.* 30:145–155.

20. Mani, J.-C., V. Marchi, and C. Cucurou. 1994. Effect of HIV-1 peptide presentation on the affinity constants of two monoclonal antibodies determined by BIAcore™ technology. *Mol. Immunol.* 31:439–444.

21. Ullén, A., B. Nilsson, K. Riklund Ahlstrom, R. Makiya, and T. Stigbrand. 1995. In vivo and in vitro interactions between idiotypic and antiidiotypic monoclonal antibodies against placental alkaline phosphatase. *J. Immunol. Methods.* 183:155–165.

22. Tello, D., E. Eisenstein, F.P. Schwarz, F.A. Goldbaum, B.A. Fields, R.A. Mariuzza, and R.J. Poljak. 1994. Structural and physicochemical analysis of the reaction between the anti-lysozyme antibody D1.3 and the anti-idiotopic antibodies E225 and E5.2. *J. Mol. Recognit.* 57–62.

23. Dighiero, G., B. Guilbert, J.P. Fermand, P. Lymberi, F. Danon, and S. Avrameas. 1983. Thirty-six human monoclonal immunoglobulins with antibody activity against cytoskeleton proteins, thyroglobulin, and native DNA: immunologic studies and clinical correlations. *Blood.* 62:264–270.

24. Carayannapoulos, L., and J.D. Capra. 1993. Immunoglobulins. Structure and function. *In* Fundamental Immunology. W.E. Paul, editor. Raven Press, New York. 283–314.

25. Strong, R.K., G.A. Petsko, J. Sharon, and M.N. Margolies. 1991. Three-dimensional structure of murine anti-p-azophenylarsonate Fab 36-71. 2. Structural basis of hapten binding and idiotypy. *Biochemistry.* 30:3749–3757.

26. Davies, D.R., S. Sheriff, and E. Padlan. 1989. Comparative study of two Fab-lysozyme crystal structures. *Cold Spring Harbor Symp. Quant. Biol.* 54: 233–238.

27. Lesk, A.M., and C. Chothia. 1988. Elbow motion in the immunoglobulins involves a molecular ball-and-socket joint. *Nature (Lond.).* 335:188–190.

28. Wilson, I.A., and R.L. Stanfield. 1994. Antibody-antigen interactions: new structures and new conformational changes. *Curr. Opin. Struct. Biol.* 4: 857–867.

29. Schneider, W.P., T.G. Wensel, L. Stryer, and V.T. Oi. 1988. Genetically engineered immunoglobulins reveal structural features controlling segmental flexibility. *Proc. Natl. Acad. Sci. USA.* 85:2509–2513.

30. Horgan, C., K. Brown, and S.H. Pincus. 1993. Studies on antigen binding by intact and hinge-deleted chimeric antibodies. *J. Immunol.* 150:5400–5407.

31. Cavacini, L.A., C.L. Emes, J. Power, M. Duval, and M.R. Posner. 1994. Effect of antibody valency on interaction with cell-surface expressed HIV-1 and viral neutralization. *J. Immunol.* 152:2538–2545.

32. Chothia, C., J. Novotny, R. Bruccoleri, and M. Karplus. 1986. Domain association in immunoglobulin molecules. The packing of variable domains. *J. Mol. Biol.* 186:651–663.

33. Padlan, E.A. 1994. Anatomy of the antibody molecule. *Mol. Immunol.* 31:169–217.

34. Bhat, T.N., G.A. Bentley, T.O. Fishmann, G. Boulot, and R.J. Poljak. 1990. Small rearrangements in structures of Fv and Fab fragments of antibody D1.3 on antigen binding. *Nature (Lond.).* 347:483–485.

35. Eigenbrot, C., M. Randal, L. Presta, P. Carter, and A.A. Kossiakoff. 1993. X-ray structures of the antigen-binding domains from three variants of humanized anti–p185HER2 antibody 4D5 and comparison with molecular modeling. *J. Mol. Biol.* 229:969–995.

36. Takahashi, H., H. Tamura, N. Shimba, I. Himada, and Y. Arata. 1994. Role of the domain–domain interaction in the construction of the antigen combining site. A comparative study by 1H-15N shift correlation NMR spectroscopy of the Fv and Fab fragments of anti–dansyl mouse monoclonal antibody. *J. Mol. Biol.* 243:494–503.

37. Van Regenmortel, M.H.V. 1989. Structural and functional approaches to the study of protein antigenicity. *Immunol. Today.* 10:266–272.